RSC Advances

PAPER

View Article Online
View Journal | View Issue

Cite this: *RSC Adv.*, 2022, **12**, 5612

Effect of fluoropolymer content on thermal and combustion performance of direct writing high-solid nanothermite composite

Yuke Jiao,[a] Shengnan Li,[a] Guoping Li *[ab] and Yunjun Luo [ab]

The addition of fluoropolymers can improve the reactivity of Al and enhance the combustion performance of thermites, which has attracted great interest. Also, direct writing 3D printing technology for the preparation of energetic materials is an innovative process that can meet a variety of complex requirements. In this study, soluble Viton F2311 was used as a binder, and F2311/Al/CuO (FMICs) nanocomposites were prepared by direct writing. The components of FMICs were evenly distributed without obvious agglomeration. The thermal and combustion properties of FMICs with different mass fractions of F2311 were systematically studied. As the F2311 content increases, the thermite reaction of FMICs is advanced and the system has a higher exothermic and combustion rate. The F2311 content had little effect on the combustion flame temperature of FMICs, all of which were above 2400 K. Compared with PTFE and new fluoropolymers/nanothermites, F2311/nanothermites shows better processability and reaction properties and probably has promising applications.

Received 10th December 2021
Accepted 25th January 2022

DOI: 10.1039/d1ra08970f

rsc.li/rsc-advances

1 Introduction

Nanothermite, also known as metastable intermixed composite (MIC), is an energetic material composed of nano-sized metal fuel (mostly Al, Mg, Ni, *etc.*) and oxide (CuO, WO_3, Fe_2O_3, *etc.*), which is a very promising reactive material with high exothermic reaction and high energy efficiency.[1] However, there are some problems with nanothermites in practical applications. (1) The nanoparticles are not uniform in size and tend to agglomerate, making them susceptible to uneven mixing during material processing and difficult to load due to their high viscosity.[2] (2) The dense oxide layer formed on the Al surface prevents contact and diffusion between the reactive Al and the oxidizer, resulting in inefficient reactions.[3] (3) Al tends to melt and agglomerate during combustion, causing incomplete combustion.[4,5] Accordingly, many approaches have been carried out to improve the processability and reactivity of nanocomposites, such as increasing the reactivity of Al,[6] preparing novel composite structures,[7] and introducing multiple components.[8,9] Among them, the introduction of fluoropolymers as binders for complexes has attracted a lot of attention. The addition of polymer binders enhances the plasticity and safety of thermites.[10] Furthermore, Yagodnikov[11] and Glotov[12] suggested that the addition of fluoropolymers could reduce the agglomeration of Al during combustion and effectively improve the combustion performance of thermites.[9,13]

In the past few decades, a series of thermite composites containing different fluoropolymers have been prepared. Huang[14] used cold-pressing and sintering technology to prepare polytetrafluoroethylene (PTFE)/Al/MoO_3 composites with a volume ratio of 60 : 16 : 24. The sample can react vigorously when impacted, with the characteristic drop height being 51.57 cm. PTFE has a high melting point (327 °C), which is close to the self-ignition temperature of nanothermites, and it is almost insoluble in any solvent. On the contrary, polyvinylidene fluoride (PVDF) and Viton can dissolve in some organic solvents, which provides more ideas for the application of nanothermites. Chen[15] added the nanothermite to PVDF polymer solution and prepared Al/MoO_3/PVDF composites by electrostatic spraying, and it was shown that the addition of PVDF could significantly reduce the reaction activation energy and contribute to the thermite reaction. The incorporation of nanothermite into polymer solutions for compounding can solve the problem of nanoparticle dispersion in composites, resulting in a more uniform distribution of material components, closer contact between fuel and oxidizer, and the composites with higher reactivity.[2,16,17] Currently, more research is focused on PTFE or PVDF/Al composites. Some novel fluoropolymers have been studied, however, due to their insoluble and refractory characteristics, the preparation of complexes is limited to high-temperature casting or ultrasonic mixing methods.[18–20] There are few studies on easily soluble fluoropolymer/nanothermite composites.

[a]*School of Materials Science and Engineering, Beijing Institute of Technology, Beijing, 100081, China. E-mail: girlping3114@bit.edu.cn*

[b]*Key Laboratory for Ministry of Education of High Energy Density Materials, Beijing Institute of Technology, Beijing, 100081, China*

The selection of the appropriate polymer and processing method is critical to the nanothermites properties. F2311 has non-toxic, good storage stability, and physical and mechanical properties. It can be dissolved in solvents such as ketones and esters with low boiling points. In the field of energetic materials, it has been combined with high-energy explosives such as HMX and CL-20 as polymer-bonded explosives.[21,22] Meanwhile, the direct writing of solvent-based inks has aroused great interest because of its relative simplicity and convenience. Moreover, the safety of energetic materials can be significantly improved with the addition of solvents.[16,17,23] Compared with traditional charging methods, such as casting and pressing of energetic materials, direct writing technology relies on its micro-nozzle and flexible arm, which has great potential advantages for micro–miniature applications of energetic materials.

In this study, soluble F2311 was selected as a fluorine-containing binder to prepare high solid content F2311/Al/CuO composites (FMICs) by direct writing. The components of FMICs are uniformly distributed and tightly combined, and there is no obvious agglomeration of nanoparticles, which provides favorable conditions for the uniform combustion of materials. The effects of F2311 content on the thermal and combustion performances of FMICs were systematically studied by thermogravimetric analysis (TGA), differential scanning calorimetry (DSC), constant volume combustion, and high-speed photography, and the combustion process of FMICs was analyzed.

2 Experimental section

2.1 Materials and chemicals

F2311 was purchased from Chenguang Chemical Research Institute. It is an elastomer made by copolymerization of vinylidene fluoride (VDF) and chlorotrifluoroethylene (CTFE). The chemical formula of F2311 is shown in Fig. 1. Butyl acetate (AR) and CuO with a diameter of 50–100 nm were purchased from Shanghai Aladdin Biochemical Technology Co., Ltd; Al nanoparticles have an average diameter of 100 nm were purchased from Shanghai Maoguo Nano Technology Co., Ltd.

2.2 Preparation of F2311/Al/CuO

According to the formulation in Table 1, F2311 was added to the butyl acetate and magnetically stirred for 3 hours to obtain a clear solution. Then the Al and CuO nanoparticles (equivalence ratio 2.0) were added to the above polymer solution and ultrasounded for 1 h to form the energetic ink. Printing was conducted with a 3D printer (Adventure Technology) using a 0.8 mm inner diameter nozzle. The print path was controlled by G-code. The speed of direct writing was 20 cm min^{-1}. The nanocomposite energetic materials were obtained by solvent volatilization and deposition. A schematic diagram of the preparation process of FMICs is shown in Fig. 2

Table 1 Energetic ink formulations with different F2311 content

Samples	F2311 (mg)	Al (mg)	CuO (mg)	Butyl acetate (g)
5% F2311 + 95% MIC	45.79	270	600	0.32
10% F2311 + 90% MIC	96.67			0.67
15% F2311 + 85% MIC	153.53			1.06
20% F2311 + 80% MIC	217.50			1.50

2.3 Characterization

The rheological properties of pure polymer solutions and highly loaded inks were tested using HAAKE rotational rheometer with a 20 mm diameter steel plate. The shear rate-viscosity test was carried out in the shear rate range from 0.01 to 100 s^{-1} at room temperature. The printing sample was observed by Hitachi SU8020 scanning electron microscope (SEM) coupled to an energy-dispersive spectrometer (EDS). The Fourier transform infrared (FT-IR) spectra of the samples were detected on a Nicolet is50 FT-IR instrument, and the ATR spectra shown here were collected at a resolution of 4 cm^{-1} and averaged over 32 scans. X-ray Photoelectron Spectroscopy (XPS) test was performed on FMICs using a PHI QUANTERA-II SXM (ULVAC-PHI, Japan) with an Al Kα source. Thermal analysis of composite materials was detected by Mettler-Toledo simultaneous thermogravimetry-differential scanning calorimeter (TGA/DSC1) at 10 °C min^{-1} heating rate under 40 ml min^{-1} Ar flow from 30 °C to 800 °C. The X-ray diffraction (XRD) test used the Rigaku Ultima IV X-ray diffractometer, a Cu target wavelength of 0.154 nm, and a scanning range of 20–100°. Constant pressure combustion test was performed with a laboratory-made closed combustion chamber (cylindrical cavity combustion chamber, Φ32 mm × 16 mm), 25 mg of samples were weighed, used American Tektronix company MDO3000 Model oscilloscope, Jiangsu Union Energy Electronic Technology Co., Ltd YE5850 model quasi-static charge amplifier to obtain the pressure signal in the reaction process. The i-SPEED 726 high-speed camera was used to record the combustion process in air, with a shutter speed of 15 000 fps and a focal length of 50 mm. The flame temperature was measured by a 50 mm METIS H3 high-speed infrared pyrometer.

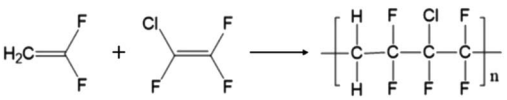

Fig. 1 Chemical composition of F2311.

Fig. 2 Diagram of preparation process of FMICs.

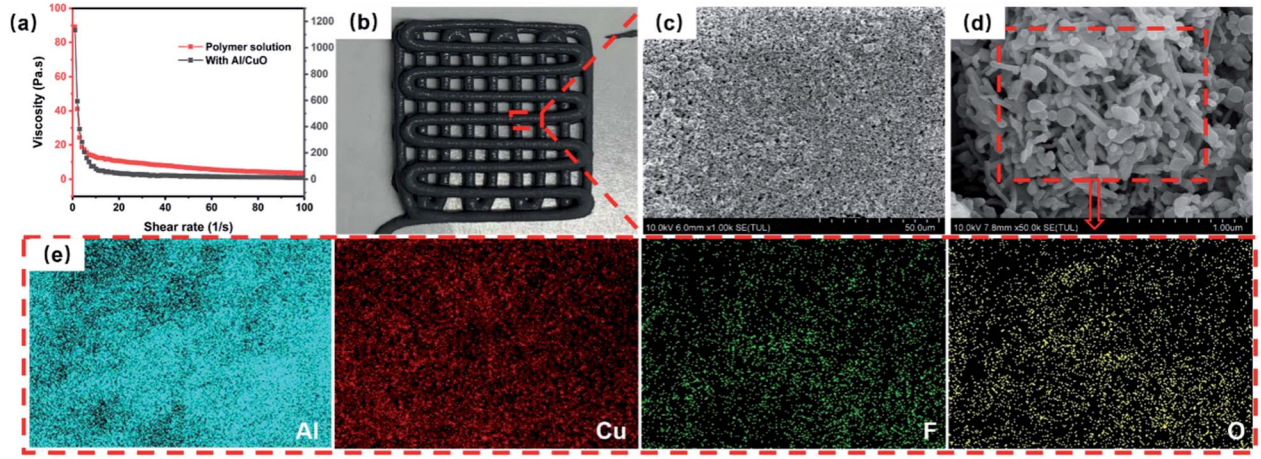

Fig. 3 (a) Apparent viscosity of polymer solutions and nanothermite ink as a function of shear rate. (b) Photograph of FMICs. (c)–(e) SEM and EDS image of the FMICs with 80 wt% Al/CuO.

3 Results and discussion

3.1 Ink rheology and characterization of FMICs

Energetic ink is a novel concept for additive manufacturing of energetic materials, which usually includes three parts: explosives or reactive materials, adhesives, and solvents. The materials that can be prepared by direct writing largely depend on the rheological properties of the prepared ink. Fig. 3a shows the dynamic shear viscosity of F2311 polymer solution and energetic ink with 80 wt% nanothermite. Both pure polymer solutions and energetic ink exhibit shear thinning characteristics. The addition of nanoparticles greatly increased the viscosity of the ink. The extremely strong shear thinning of the ink made it similar to the viscosity of the polymer at high shear rates. This feature is very suitable for direct writing of pass through millimeter or even micron nozzles under certain pressure conditions.[2,16,24]

Fig. 3b is the photograph of FMICs by direct writing. Fig. 3c and d show low and high magnification SEM images of the surface of the double-layer FMICs. The F2311 binder was tightly wrapped with the nanothermite to provide a self-supporting structure for the composite material. At the same time, the Al and CuO nanoparticles were tightly assembled. From the EDS results of each element (Fig. 3e), it can be seen that the components of the FMICs obtained by direct writing were uniformly distributed, and there was no obvious agglomeration phenomenon between the nanoparticles.

The elements composition of FMICs was analyzed by XPS. Fig. 4a shows the survey spectrum of the surface of FMICs, which clearly shows that FMICs contain C, O, F, Cu, and Al elements. The high-resolution XPS spectra of FMICs was further fitted with Gaussian, and the result is shown in Fig. 4b. The results correspond to C–C, C–F, and CF_2 at 285.0 (±0.2) eV, 287.0 (±0.2) eV, and 291.4 (±0.2) eV, respectively. Fig. 4c shows the FTIR spectra of F2311 and FMICs. The $-CF_2$ stretching vibration peak of FMICs is shifted toward the lower wavenumber due to the intermolecular hydrogen bonding between C–F on the molecular chain of F2311 and –OH on the surface of

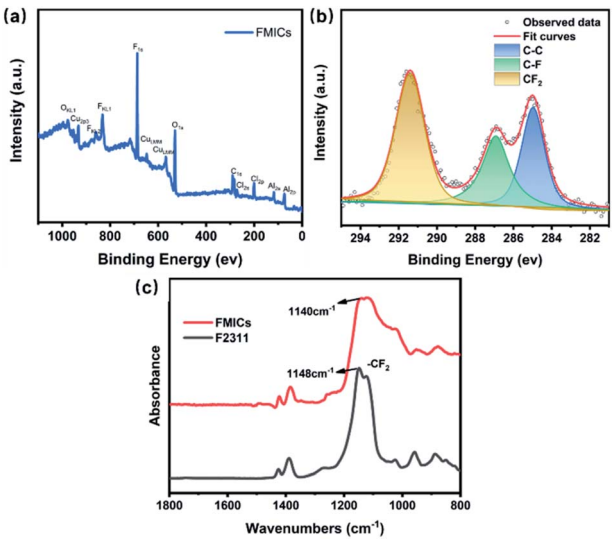

Fig. 4 (a) Survey spectrum of FMICs, (b) C 1s spectrum of FMICs, (c) FTIR spectra of F2311 and FMICs.

nano Al and CuO. It indicates that there is an interaction between F2311 and nano-Al thermite, which is beneficial to the long-term storage of the ink.

3.2 Thermal analysis of FMICs with different F2311 content

To study the thermal properties and combustion reaction process of nanocomposites, TG-DSC thermal analysis of FMICs with different F2311 contents were characterized, and the combustion products were analyzed by XRD. The results are shown in Fig. 5 and Fig. 6.

The TG-DTG results (Fig. 5a and b) indicated that the thermal decomposition process of FMICs can be divided into three stages. The first stage (100–300 °C) mainly removes small molecules such as water and organic solvents adsorbed on the surface of the material during the preparation and storage of

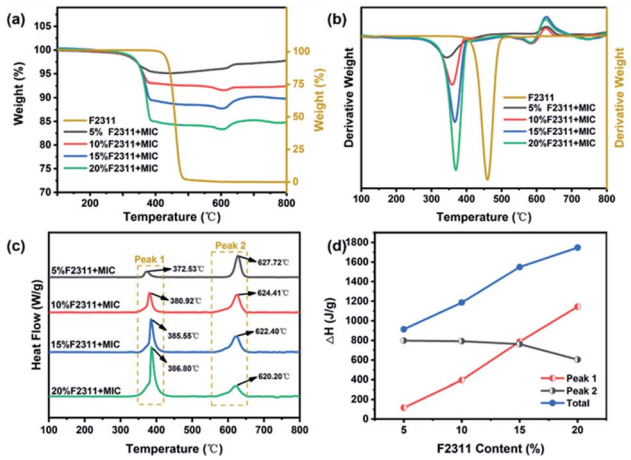

Fig. 5 (a) TG curve, (b) DTG curve, (c) DSC curve, (d) heat release of FMICs with different F2311 contents.

FMICs. The second stage (300–385 °C) is the F2311 thermally decomposes (the weight loss is related to the F2311 content of the composite, which is about 97 wt% of the F2311) and reacts with the Al_2O_3 shell on the surface of Al and releases an amount of heat (Fig. 5c peak 1 low-temperature section). At this point, the oxide layer is destroyed, the reactive Al is exposed to the binder and oxidizer and the fluorination of the Al takes place, releasing a large amount of heat (Fig. 5c peak 1 high-temperature section). This process is known as the pre-ignition reaction (PIR), which is shown in eqn (1) and (2).

Pre-ignition reaction:

$$Al_2O_3 + F2311 \rightarrow AlF_3 + heat \quad (1)$$

$$Al + F2311 \rightarrow AlF_3 + heat \quad (2)$$

According to the thermal weight-loss parameters in Table 2, the decomposition temperature of FMICs are lower than that of pure F2311 polymer. The addition of nanothermite can facilitate the thermal decomposition of F2311. When the mass fraction of nanothermite increases from 80% to 95%, the DTG peak temperature of F2311 decreased by about 92–118 °C, and the peak temperature of fluorination reaction decreased by 14.27 °C. The decrease in decomposition temperature of F2311 can be attributed to the PIR, which can also be observed in the reaction of Al with PTFE, PVDF, and other fluoropolymers.[18,25,26] It can be seen from Fig. 5c peak 1 that with the increasing content of F2311, the more heat released from fluorination reaction, the higher the total heat released from FMICs. When the mass fraction of F2311 increased from 5% to 20%, the total heat increased from 913.18 J g^{-1} to 1747.19 J g^{-1}. F2311 is capable of PIR with Al and Al_2O_3 shell layer, and the reaction product AlF_3 sublimates at 1277 °C, which makes the system internally pressurized while the particles break up and reduce

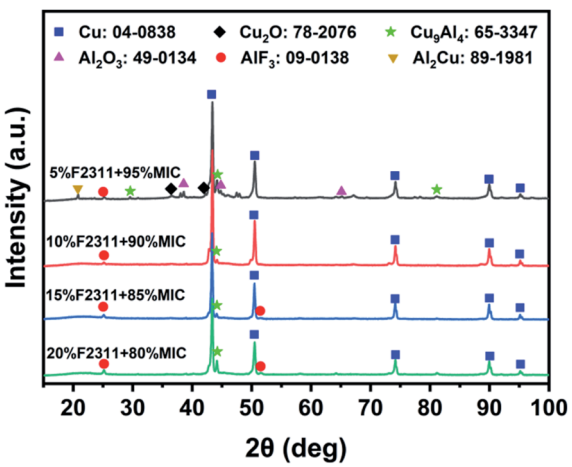

Fig. 6 XRD of the combustion products of FMICs with different contents.

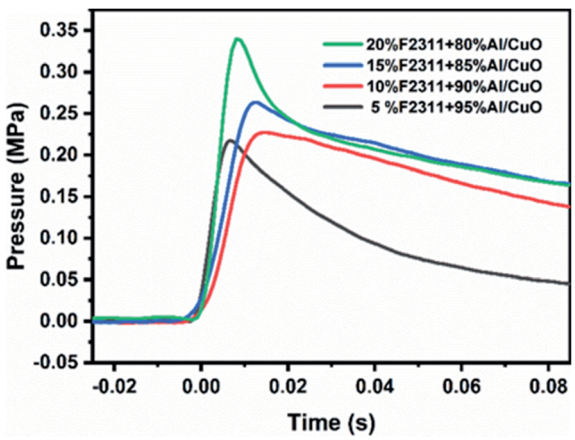

Fig. 7 *P–t* curve of FMICs with different F2311 contents.

Table 2 Thermal weight-loss parameters of FMICs with different F2311 contents

Samples	DTG peak temperature (°C)	Peak 1		Peak 2		Total heat
		Peak temperature (°C)	ΔH (J g^{-1})	Peak temperature (°C)	ΔH (J g^{-1})	ΔH (J g^{-1})
5% F2311 + 95% MIC	343.23	372.53	115.49	627.72	797.69	913.18
10% F2311 + 90% MIC	359.28	380.92	394.66	624.41	791.89	1186.55
15% F2311 + 85% MIC	366.70	385.55	786.34	622.40	762.01	1548.35
20% F2311 + 80% MIC	369.56	386.80	1143.34	620.20	603.85	1747.19
F2311	461.54	—	—	—	—	—

agglomeration. The incorporation of F2311 contributed to the higher reaction energy and better combustion properties of the nanothermite composites.[9,13,27]

The third stage (385–580 °C) is the further decomposition of F2311 polymer, and the weight loss rate is about 3 wt% of F2311 in FMICs. The increase in mass (above 600 °C) is since although the argon atmosphere is used for purging, there is inevitably a trace of air in the furnace cavity, which reacts with Al under high-temperature conditions. When the temperature is higher than 600 °C, FMICs undergo the thermite reaction and release heat (Fig. 5c peak 2), as shown in eqn (4), as the content of F2311 increases, the thermite reaction advances.

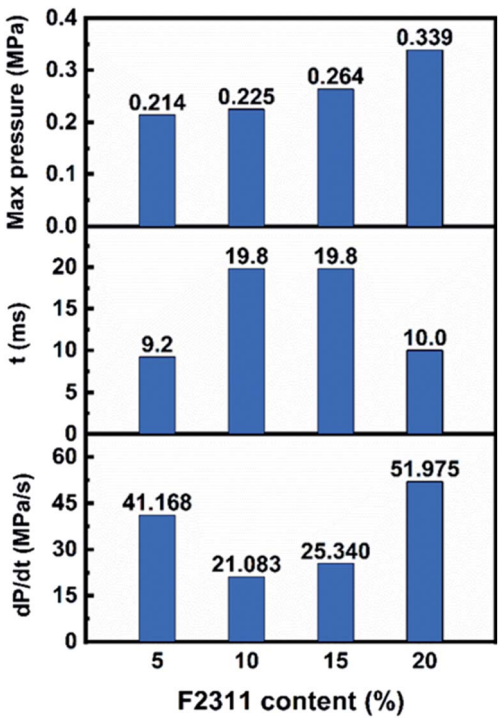

Fig. 8 *P–t* curve parameters of FMICs with different F2311 contents.

The XRD results in Fig. 6 show that the combustion product of 5 wt% F2311 contains Cu_2O and relatively more Cu_9Al_4 compared to other mass fractions of F2311. It is reported that Cu_9Al_4 is a product in the fuel-rich Al/CuO nanothermite composites, which is formed by the reaction of excess Al and Cu_2O, as shown in eqn (4) and (5).[18,28] FMICs with F2311 content above 5 wt% recorded the lowest relative peak intensity for Al_2O_3 with respect to AlF_3, which indicates that fluorination is the dominant mechanism for Al consumption over oxidation. This is also consistent with the stronger peak intensities observed for the PIR in the DSC result (Fig. 5c).

Thermite reaction:

$$2Al + 3CuO \rightarrow Al_2O_3 + 3Cu \quad (3)$$

$$2Al + 6CuO \rightarrow Al_2O_3 + 3Cu_2O \quad (4)$$

$$Al + 9Cu_2O \rightarrow 3Al_2O_3 + 2Cu_9Al_4 \quad (5)$$

3.3 Constant volume combustion performance of FMICs

The pressure–time curves (*P–t* curves) for FMICs were obtained by using a constant-volume combustion chamber equipped with a pressure sensor, as shown in Fig. 7. It can be observed that the pressure profiles of FMICs with different F2311 content progress smoothly over time without any oscillation, indicating that the nanoparticles were uniformly dispersed in the F2311 binder matrix.[18]

All samples showed a process of sharp increase and gradual decay in the pressure curves. The increase in pressure can be attributed to the following factors: (1) the heat released during combustion increases the temperature of the gas in the combustion chamber. (2) The combustion process forms shock waves at the high temperature and pressure reaction. (3) Gas products: the adiabatic temperature of the thermite reaction is higher than the boiling point of Al (2327 °C), so the part of Al vaporizes during the reaction; in the presence of F2311, Al is not only oxidized by CuO but also undergoes fluorination reaction

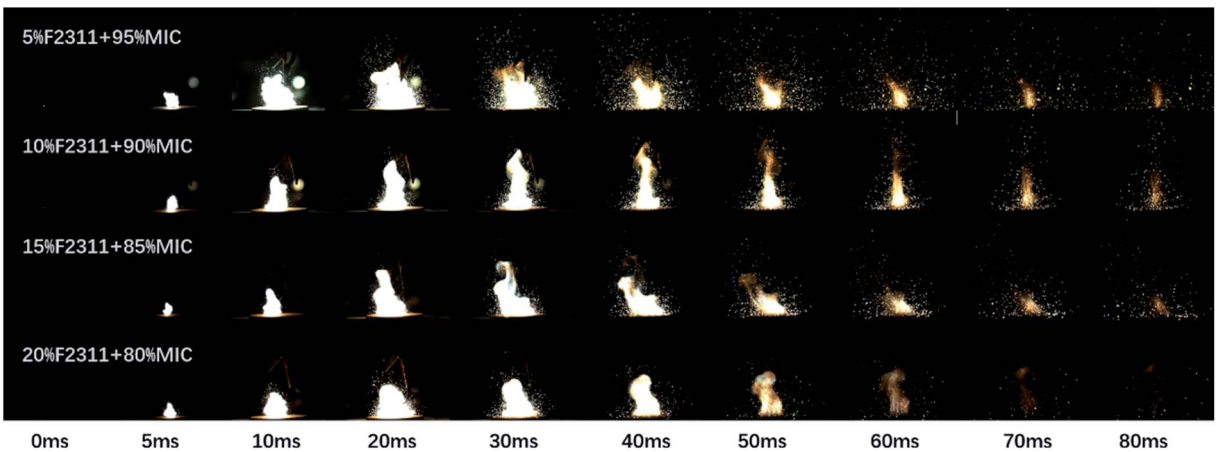

Fig. 9 High-speed photographs of the combustion process of FMICs with different F2311 contents.

with F2311 to produce gaseous AlF_3. In addition, the binder will generate several fluorine-containing gases.

Typically, the maximum pressure generated (P_{max}) represents the release of reaction energy; the time to reach P_{max} and the pressure rise rate (dP/dt) are indicators for the reactivity of the energetic material. The parameters of the P–t curves of FMICs with different F2311 content are shown in Fig. 8. P_{max} tends to increase with increasing F2311 content. This is consistent with the pattern of exothermic values of FMICs reported in the previous section. The addition of more F2311 causes FMICs to generate more heat and gaseous products during combustion, which leads to a higher P_{max}. The binder hinders the propagation of heat, which affects the reactivity of the material. Therefore 5 wt% F2311 composites showed relatively high reactivity ($dP\ dt^{-1}$). Favorably, the PIR occurring between the fluoropolymer and Al particles provides the additional heat. When the F2311 content is 10 wt% or more, the PIR reaction is more intense, and more heat is released as the F2311 content increases, so the reactivity increases accordingly. When the mass fraction of F2311 reached 20%, the positive effect from PIR was greater than the negative effect from the binder, thus improving the overall reactivity.

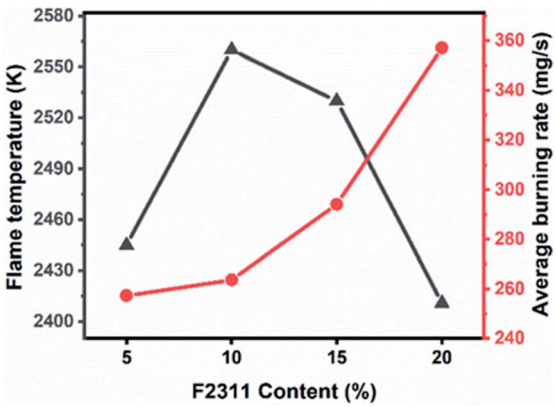

Fig. 10 Flame temperature and burning rate of FMICs with different F2311 contents.

3.4 Combustion process of FMICs

The combustion process of FMICs under normal pressure was recorded by high-speed photography. Fig. 9 is a series of high-speed photographs showing FMICs of the same mass (25 mg) ignited by Ni–Cr wire in the atmosphere. It can be observed that the burning duration of FMICs were within 100 ms, the flame was bright yellow, and the closer to the burning surface, the greater the flame brightness; there are splashed particles in the gas phase region, which was because the gaseous substances generated during the combustion of FMICs bring them into the gas phase region and continue to burn fully. Taking the first screen where the burning bright spot appears as the zero moment, as the F2311 content decreases, the shorter the time for FMICs to reach the most intense burning. Because according to the TG curve we understand that the thermite can facilitate the decomposition of F2311, thereby promoting the pre-ignition reaction; While with the increase of F2311 content, FMICs can burn out faster and have higher burning rate. The flame temperature was measured by infrared thermometer, and the results are shown in Fig. 10. The mass fraction of F2311 had little effect on the flame temperature of FMICs, which were all higher than 2400 K.

Table 3 summarizes the thermal and combustion properties of PTFE, PVDF, and novel fluoropolymer compounded with nanothermites reported in the literature in recent years. All these fluoropolymers have PIR and thermal reaction processes. Among them, F2311/nanothermites composites have more obvious advantages in terms of heat release as well as combustion rate. For example, F2311/nanothermites exerts 87% to 353% more heat than PTFE and PVDF-based composites. In addition, compared with PTFE and other novel fluoropolymer, they are mostly prepared by ultrasonic mixing due to their insolubility and high melting point. F2311 is easily soluble in

Table 3 Comparison of thermal and combustion properties of other fluoropolymer/nano-thermite composites

		PIR		Thermite reaction				
Samples	Preparation	peak temperature (°C)	ΔH (J g^{-1})	peak temperature (°C)	ΔH (J g^{-1})	Total heat (J g^{-1})	P_{max} (MPa g^{-1})	Burn rate (mg s^{-1})
30%PVDF/Al/MoO_3 (ref. 15)	Electrospraying	448.1	162.7	680.1	771.3	934.0	—	228.0
20%PVDF/Al/CuO[29]	Electrospinning	360, 460	—	About 610	—	—	—	—
30%PTFE/Al/MnO_2 (ref. 30)	Ultrasonic mixing	500–650	176.1	About 750	209.1	385.2	—	—
30%PTFE/Al/MoO_3 (ref. 31)	Ultrasonic mixing	568.0	255.7	About 660	—	—	—	—
40%FP/Al/CuO[18]	Cast curing	348.0	—	About 600	—	880.0	0.6	348.0
20%PFPE/Al/CuO[20]	Evaporative deposition	303.0	51.4	583.0	843.0	894.4	—	—
20%PFPE/Al/MoO_3 (ref. 20)	Evaporative deposition	305.0	103.1	566.0	1889.0	1992.1	—	—
20%F2311/Al/CuO	Direct writing	386.8	1143.3	620.2	603.9	1747.2	13.6	358.0

organic solvents, thus F2311/nanothermites composites could have a greater potential for application.

4 Conclusions

(1) The nanocomposite energetic materials were successfully prepared by direct writing. SEM and EDS showed that the components of FMICs were uniformly distributed. (2) The thermal properties of F2311 and FMICs were studied by TG-DSC. Nanothermite can facilitate the decomposition of F2311. With the increase of F2311 content, the PIR releases more heat, the thermite reaction advances, and the total energy of the system increases. When the mass fraction of F2311 increased from 5% to 20%, the heat exotherm of PIR increased by 890.00%, the total heat exotherm of the system increased by 91.33%, and the peak temperature of the thermite reaction decreased by 7.52 °C. (3) The combustion products of FMICs were analyzed by XRD. The nanothermite composites with a mass fraction of 5–20% F2311 (the equivalent ratio of the thermite is 2.0) is a fuel-rich system. When the mass fraction of F2311 is greater than 5%, the fluorination of Al is the main mechanism for consuming Al. (4) The combustion performance of FMICs was characterized by a closed combustion chamber and high-speed photography. The maximum pressure produced by combustion rose with the increase of F2311 content, and the appropriate addition of F2311 could improve the reaction activity of FMICs. The combustion process of FMICs with different F2311 mass fractions is within 100 ms, and with the increase of F2311 content, the average combustion rate is faster, while the time to reach the strongest combustion is longer.

Conflicts of interest

There are no conflicts to declare.

Acknowledgements

This work was financially supported by NSFC and State Administration of Science, Technology and Industry for National Defense of China (HYZ2018001).

Notes and references

1 R. A. Williams, M. Schoenitz and E. L. Dreizin, *Combust. Sci. Technol.*, 2014, **186**, 47–67.
2 H. Wang, J. Shen, D. J. Kline, N. Eckman, N. R. Agrawal, T. Wu, P. Wang and M. R. Zachariah, *Adv. Mater.*, 2019, **31**, e1806575.
3 S. Valluri, M. Schoenitz and E. Dreizin, *Def. Technol.*, 2019, **15**, 1–22.
4 P. F. Pokhil, V. S. Logachev and V. M. Mal'Tsev, *Combust., Explos. Shock Waves*, 1970, **6**, 76–85.
5 L. Liang, X. Guo, X. Liao and Z. Chang, *Appl. Surf. Sci.*, 2020, **508**, 144790.
6 W. Yi, J. Wei, L. Lixin, L. Hongying, L. Yaqing and L. Fengsheng, *Rare Met. Mater. Eng.*, 2012, **41**, 9–13.
7 H. Yang, G. Yang, X. Li, H. Bao, Y. Yang, X. Guo, Z. Qiao and X. Li, *J. Alloys Compd.*, 2021, **877**, 160025.
8 E.-C. Koch, *Propellants, Explos., Pyrotech.*, 2002, **27**, 340–351.
9 H. Wang, M. Rehwoldt, D. J. Kline, T. Wu, P. Wang and M. R. Zachariah, *Combust. Flame*, 2019, **201**, 181–186.
10 W. He, P.-J. Liu, F. Gong, B. Tao, J. Gu, Z. Yang and Q.-L. Yan, *ACS Appl. Mater. Interfaces*, 2018, **10**, 32849–32858.
11 D. A. Yagodnikov, E. A. Andreev, V. S. Vorob'Ev and O. G. Glotov, *Combust., Explos. Shock Waves*, 2006, **42**, 534–542.
12 O. G. Glotov, D. A. Yagodnikov, V. S. Vorob'Ev, V. E. Zarko and V. N. Simonenko, *Combust., Explos. Shock Waves*, 2007, **43**, 320–333.
13 T. R. Sippel, S. F. Son and L. J. Groven, *Propellants, Explos., Pyrotech.*, 2013, **38**, 286–295.
14 J. Huang, X. Fang, S. Wu, L. Yang, Z. Yu and Y. Li, *Materials*, 2018, **11**, 1200.
15 J. Chen, T. Guo, M. Yao, J. Song, W. Ding, Y. Mao, S. Li and R. Zhu, *Mater. Res. Express*, 2020, **7**, 115009.
16 J. Shen, H. Wang, D. J. Kline, Y. Yang, X. Wang, M. Rehwoldt, T. Wu, S. Holdren and M. R. Zachariah, *Combust. Flame*, 2020, **215**, 86–92.
17 H. Woods, A. Boddorff, E. Ewaldz, Z. Adams, M. Ketcham, D. J. Jang, E. Sinner, N. Thadhani and B. Brettmann, *Propellants, Explos., Pyrotech.*, 2019, **45**, 26–35.
18 H. Nie, L. P. Tan, S. Pisharath and H. H. Hng, *Chem. Eng. J.*, 2021, **414**, 128786.
19 J. Wang, Y. Qu, F. Gong, J. Shen and L. Zhang, *Combust. Flame*, 2019, **204**, 220–226.
20 J. McCollum, M. L. Pantoya and S. T. Iacono, *ACS Appl. Mater. Interfaces*, 2015, **7**, 18742–18749.
21 G.-Y. Hang, W.-L. Yu, T. Wang and Z. Li, *J. Mol. Model.*, 2018, **24**, 97.
22 J. Xiao, W. Zhu, X. Ma, H. Xiao, H. Huang and J. Li, *Mol. Simul.*, 2008, **34**, 775–779.
23 F. D. Ruz-Nuglo and L. J. Groven, *Adv. Eng. Mater.*, 2018, **20**, 1700390.
24 Y. Mao, L. Zhong, X. Zhou, D. Zheng, X. Zhang, T. Duan, F. Nie, B. Gao and D. Wang, *Adv. Eng. Mater.*, 2019, **21**, 1900825.
25 H. Nie, S. Pisharath and H. H. Hng, *Combust. Sci. Technol.*, 2020, 1–17, DOI: 10.1080/00102202.2020.1813119.
26 K. S. Kappagantula, C. Farley, M. L. Pantoya and J. Horn, *J. Phys. Chem. C*, 2012, **116**, 24469–24475.
27 R. Padhye, A. J. A. Aquino, D. Tunega and M. L. Pantoya, *ACS Appl. Mater. Interfaces*, 2017, **9**, 24290–24297.
28 D. Stamatis, Z. Jiang, V. K. Hoffmann, M. Schoenitz and E. L. Dreizin, *Combust. Sci. Technol.*, 2008, **181**, 97–116.
29 X. Li, C. Huang, H. Yang, Y. Li and Y. Cheng, *J. Therm. Anal. Calorim.*, 2016, **124**, 899–907.
30 J. Zhang, J. Huang, X. Fang, Y. Li, Z. Yu, Z. Gao, S. Wu, L. Yang, J. Wu and J. Kui, *Materials*, 2018, **11**, 2451.
31 J. Wu, B. Feng, Z. Gao, Y. Li, S. Wu, Q. Yin, J. Huang and X. Ren, *J. Fluorine Chem.*, 2021, **241**, 109676.